

EFFECTS OF STOICHIOMETRIC RATIO ON STRUCTURE AND ELECTRODE PERFORMANCE OF HYDROGEN STORAGE ALLOYS^①

Chen Weixiang

*Department of Materials Science and Engineering,
Zhejiang University, Hangzhou 310027, P. R. China*

ABSTRACT The effects of stoichiometric ratio x on the structure, thermodynamic properties and electrode performances of the hydrogen storage alloys $Mm(Ni_{0.72}Co_{0.14}Mn_{0.08}Al_{0.06})_x$ ($Mm = Ce$ -rich mischmetal, $x = 4.4 \sim 5.0$) were studied. The major phases of all alloys are of hexagonal $CaCu_5$ type structure. The unit cell volume increases with decreasing stoichiometric ratio x . A small quantity of the second phase Ce_2Ni_7 is segregated in the alloy with $x < 5.0$ and the amount of Ce_2Ni_7 phase increases with decreasing x . The enthalpy change $-\Delta H$ value of hydride formation increases with decreasing x because of increasing unit cell volume and the Ce_2Ni_7 phase forming more stable metal hydride. The discharge capacities of MH electrodes increase with increasing x but for alloy with $x = 5.0$, and have a maximum 306 mAh/g at $x = 4.8$. The exchange current density of MH electrode reaction increases but the high rate dischargeability decreases with decreasing x . This fact indicated that the hydrogen diffusion in the alloy is a rate-determining step in high rate discharging.

Key words hydrogen storage alloy stoichiometric ratio structure thermodynamic property

1 INTRODUCTION

Nickel-metal hydride (Ni/MH) batteries employing a hydrogen storage alloy as the negative material have attracted much attention because they have higher energy density, better tolerance to over-charge/over-discharge and free from cadmium compared with the conventional Ni/Cd batteries. Many multicomponent mischmetal-based hydrogen storage alloys have been developed to improve performances of Ni/MH batteries^[1-3]. In addition, MH electrodes performances such as capacity, activation property, electrocatalytic activity were also effectively improved by surface modifications of hydrogen storage alloy or MH electrodes^[4,5] and adding metal and metal oxide to MH electrodes^[6,7].

Recently, the research about the effects of stoichiometric ratio on the thermodynamic properties and MH electrodes performances of hydro-

gen storage alloys were carried out. Nogami^[8] first reported the nonstoichiometric alloys with a composition of $Mm(NiCoMnAl)_{4.55 \sim 4.76}$ showed higher discharge capacity than stoichiometric alloy $Mm(NiCoMnAl)_5$. Notten^[9] found that the electrocatalytic activities of superstoichiometric hydrogen storage alloys $La_{0.8}Nd_{0.2}Ni_{3.0}Co_{2.4}Si_{0.1}$ and $La_{0.8}Nd_{0.2}Ni_{2.9}Co_{2.4}Mo_{0.1}Si_{0.1}$ were higher than that of $La_{0.8}Nd_{0.2}Ni_{2.5}Co_{2.4}Si_{0.1}$. Nogami^[10] also found that high rate discharge characteristics of $MmNi_5$ -type hydrogen storage alloys electrodes were greatly improved by adding such elements as boron, molybdenum, tantalum and zirconium. Especially, the addition of boron and molybdenum were more effective on discharge capacity.

The nonstoichiometric hydrogen storage alloy was confirmed to be a new type negative material with high performance for Ni/MH battery. These nonstoichiometric alloys consisted of

① Project 863-715-004-0060 supported by the National Advanced Materials Committee of China

Received Sep. 15, 1997; accepted Nov. 25, 1997

two or more phases and had good electrocatalytic activity. In this paper, the effects of stoichiometric ratio x on the structure, thermodynamic properties of $Mm(Ni_{0.72}Co_{0.14}Mn_{0.08}Al_{0.06})_x$ ($x = 4.4 \sim 5.0$) and electrodes performances were investigated. The relationships between their electrochemical performances and structure were discussed.

2 EXPERIMENTAL DETAILS

The alloys $Mm(Ni_{0.72}Co_{0.14}Mn_{0.08}Al_{0.06})_x$ ($Mm = Ce$ -rich mischmetal, La: 28.3%, Ce: 55.0%, Pr: 5.4%, Nd: 15.9%; $x = 4.4, 4.6, 4.8, 5.0$) were prepared by arc melting under argon atmosphere. The purities of the constituent metals were above 99.9% but for mischmetal. The alloys in the as-cast state were crushed mechanically to $74 \sim 50 \mu m$.

Crystal structure and lattice parameters of the alloys were determined by powder X-ray diffraction (XRD) using D/MAX-III A X-ray diffractometer with $CuK\alpha$ radiation and a graphite diffracted-beam filter. Pressure composition isothermals (P-C-T) curves for the hydrogen storage alloy were measured at different temperatures by electrochemical method. Both the enthalpy change (ΔH) and entropy change (ΔS) of hydride formation are calculated from the plateau pressures of alloys at different temperatures by following Van't Hoff equation,

$$\ln p_{eq} = \frac{\Delta H}{RT} - \frac{\Delta S}{R} \quad (1)$$

MH electrodes were prepared by cold pressing the mixtures of hydrogen storage alloy powders ($74 \sim 50 \mu m$) with electrolytic copper powder ($50 \mu m$) in the mass ratio of 1:2 at 18 MPa to form 10 mm diameter pellets. Electrochemical measurements were carried out in open glass cell. The sintered nickel hydroxide electrode having electrochemical capacity much larger than that of MH electrode was used as counter electrode. The reference electrode was a Hg/HgO (KOH 6 mol/L) electrode. The electrolyte was a KOH 6 mol/L solution. Galvanostatic charge-discharge cycling test was performed at room temperature. MH electrode was charged for 4 h and discharged to 0.6 V vs Hg/HgO after a rest

of 5 min at a constant current density of 100 mA/g. The high-rate dischargeability was determined from the ratio of the discharge capacity measured at 1250 mA/g to that at 100 mA/g. The exchange current density (J_0) was measured nearly equilibrium potential ($\varphi_e \pm 10$ mV) by the linear sweep voltammetry (LSV) at a scan rate of 1 mV/s (Solartron 1286 electrochemical interface) at different depth of charge (DOC). In order to measure the charge retention (C_R) of the alloy electrode, MH electrode was charged for 4 h at 100 mA/g. It discharged at 100 mA/g after standing for 48 h at 298 K in open cell. The charge retention was defined by following equation.

$$C_R = C_2 / C_1 \times 100\%$$

where C_1 is the discharge capacity measured before standing, C_2 is the discharge capacity measured after standing for 48 h.

3 RESULTS AND DISCUSSION

3.1 Crystallographic and thermodynamic properties of hydrogen storage alloys

The XRD spectra of hydrogen storage alloys are shown in Fig. 1. It is found that hydrogen storage alloy of $x = 5.0$ has single phase with hexagonal $CaCu_5$ type structure. The XRD patterns of alloys with $x < 5.0$ show additional XRD peaks attributed to Ce_2Ni_7 phase besides the peaks corresponding to the major phase of $CaCu_5$ type. Therefore, the nonstoichiometric alloys ($x < 5$) have double phases with $CaCu_5$ type structure as major phase and a small quantity of Ce_2Ni_7 as the second phase. Lattice parameter (a , c) and unit cell volume (V) of hydrogen storage alloy are calculated by means of following eqns.,

$$\frac{1}{d^2} = \frac{3}{4} \cdot \frac{h^2 + h \cdot k + k^2}{a^2} + \frac{l^2}{c^2} \quad (2)$$

$$V = \frac{\sqrt{3}}{2} \cdot a^2 \cdot c \quad (3)$$

The content of the second phase Ce_2Ni_7 would be calculated from the ratio of intensity of peak of Ce_2Ni_7 phase to that of major phase. The results are listed in Table 1.

According to Table 1, the unit cell volume

of the alloys increases with stoichiometric ratio x decreasing because the atom radius of mischmetal are larger than that of Ni, Mn, Co and Al, and the content of Ce_2Ni_7 phase in the alloys increases with stoichiometric ratio x decreasing.

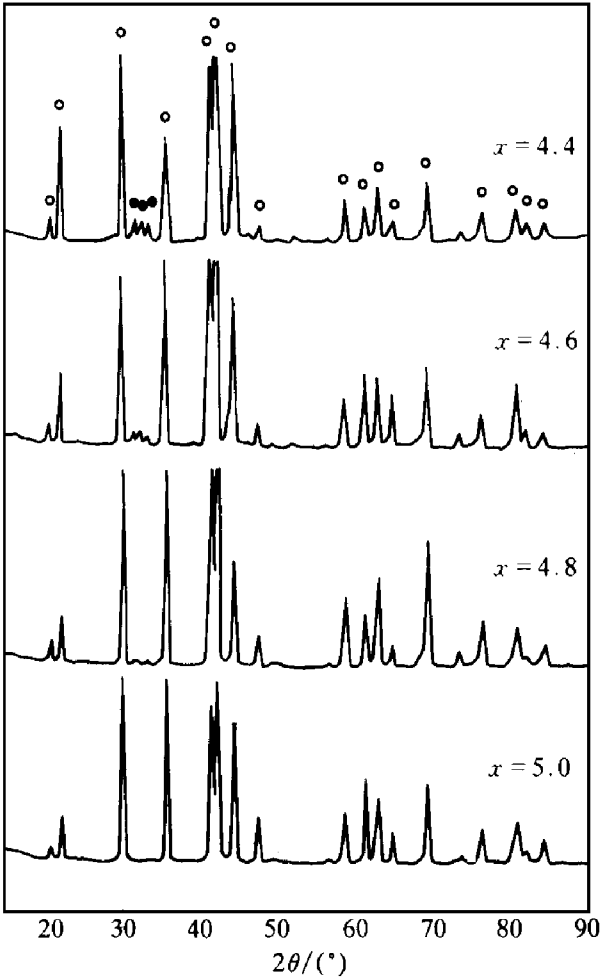


Fig. 1 XRD spectra of hydrogen storage alloys
○— CaCu_5 phase; ●— Ce_2Ni_7 phase

Table 1 Effect of x on unit cell volume and content of Ce_2Ni_7 phase of alloys

Alloys MmB_x	Unit cell volume/ \AA^3	Content of Ce_2Ni_7 / %
$x = 5.0$	86.53	0.0
$x = 4.8$	86.74	2.07
$x = 4.6$	86.89	3.60
$x = 4.4$	86.95	7.04

Fig. 2 is the Van' t Hoff curves of the alloys. It is found that the equilibrium pressure (p_{eq}) decreases with stoichiometric ratio x decreasing at the same temperature. Table 2 is the

effect of stoichiometric ratio x on enthalpy change (ΔH) and entropy change (ΔS) of metal hydride formation of hydrogen storage alloys. The $-\Delta H$ value increase with x decreasing because of the unit cell volume increasing and the Ce_2Ni_7 phase forming more stable metal hydride.

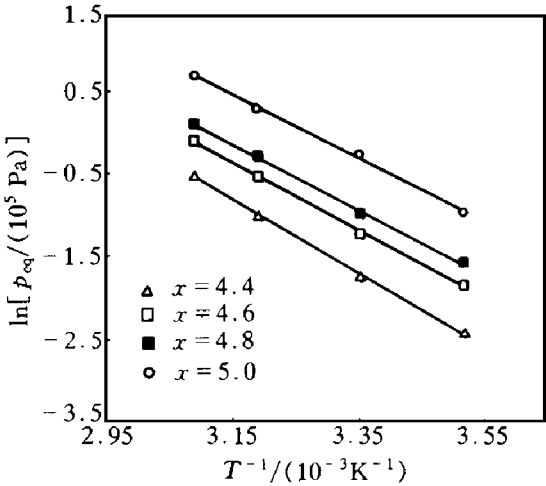


Fig. 2 Van' t Hoff curves of alloys

Table 2 Effect of x on ΔH and ΔS of metal hydride formation of alloys

Alloy MmB_x	ΔH / ($\text{kJ}\cdot\text{mol}^{-1}$)	ΔS / ($\text{J}\cdot\text{mol}^{-1}\cdot\text{K}^{-1}$)	p_{eq} / (298 K) Pa
$x = 5.0$	- 32.5	- 105.8	77.3×10^3
$x = 4.8$	- 33.2	- 103.8	37.3×10^3
$x = 4.6$	- 34.1	- 104.6	29.6×10^3
$x = 4.4$	- 36.7	- 109.0	17.7×10^3

3.2 Effects of stoichiometric ratio x on electrodes performances of alloys

3.2.1 Discharge capacities of MH electrodes

Activation curves for the hydrogen storage alloys electrodes are shown in Fig. 3. It is found that the nonstoichiometric alloys ($x < 5.0$) electrodes have better activation property than stoichiometric alloy ($x = 5.0$) electrode. For the alloys with $x < 5.0$, MH electrodes are almost completely activated within 3rd– 4th cycle, for the alloy with $x = 5.0$, MH electrode isn't completely activated untill 8th cycle. The fact is caused by that a small amount of the second phase Ce_2Ni_7 segregated in the alloy with $x < 5.0$ has higher electrocatalytic activity for electrode reaction to improve the activation prop

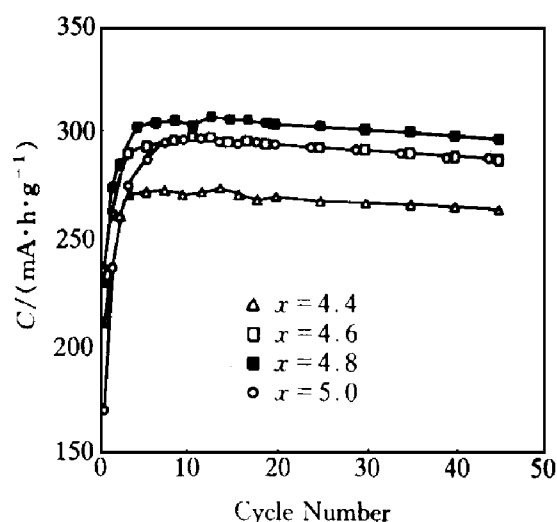


Fig. 3 Activation curves of hydrogen storage alloys electrodes

erty of MH electrode.

From Table 3, the discharge capacities of the alloys increase with x increasing but for alloy with $x = 5.0$ and have a maximum of 306 mA/h/g at $x = 4.8$. In general, from table 3 and 1 the discharge capacity of hydrogen storage alloy increases with unit cell volume increasing. The unit cell volumes of the alloys with $x = 4.4$ and 4.6 are larger than that of alloy with $x = 4.8$, but their discharge capacities are less than that of the alloy with $x = 4.8$. Because a part of hydrogen with Ce_2Ni_7 phase forms more stable metal hydride and the part of capacity wouldn't be completely discharged to result in reduction in discharge capacity.

3.2.2 High rate dischargeability and electrocatalytic activity of MH electrodes

As listed in Table 4, the high rate dischargeability of the alloy electrodes reduced with x decreasing.

The exchange current densities of MH electrodes at different depths of charge (DOC) are shown in Fig. 4. The exchange current densities increase markedly with DOC increasing in a region of α -phase ($\text{DOC} < 30\%$). Further charging, the exchange current densities have no large change in the $\alpha + \beta$ two-phase region ($30\% < \text{DOC} < 80\%$). The exchange current densities in signal β -phase region ($\text{DOC} > 85\%$) are lower slightly than that in $\alpha + \beta$ two-phase region. The

exchange current densities of the alloys electrodes (in $\alpha + \beta$ two-phase region) increase with stoichiometric ratios x decreasing. It is caused by the fact that the amount of Ce_2Ni_7 phase with higher electrocatalytic activity in the alloys increased with x decreasing. The relationship

Table 3 Effect of x on discharge capacities of MH electrodes

Alloys MmB_x	Discharge capacity/(mA·h·g ⁻¹)
$x = 4.4$	274.2
$x = 4.6$	298.1
$x = 4.8$	306.1
$x = 5.0$	296.4

Table 4 High rate dischargeability of alloy electrodes

MmB_x	HRD/ %
$x = 4.4$	43.4
$x = 4.6$	57.6
$x = 4.8$	66.3
$x = 5.0$	75.2

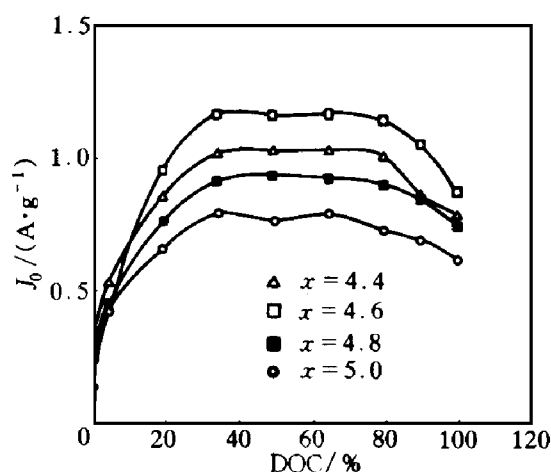


Fig. 4 Exchange current density(J_0) of MH electrodes at different depth of charge(DOC)

between high rate dischargeability and exchange current density of MH electrode is shown in Fig. 5. If the electron transfer on the electrode surface was the rate-determining step, the high rate dischargeability would increase with increasing the exchange current density. But according to

Fig. 5, the high rate dischargeability of the alloy electrode decreases with the exchange current density J increasing. Therefore, it is believed that the hydrogen diffusion in the alloy is rate determining step in high rate discharging. The larger the enthalpy change $-\Delta H$ value of metal hydride formation is, the more difficult the hydrogen diffusion in bulk of the alloy is. So that the $-\Delta H$ value increases with x decreasing, the hydrogen diffusion gets more difficult to result in reduction in high rate dischargeability.

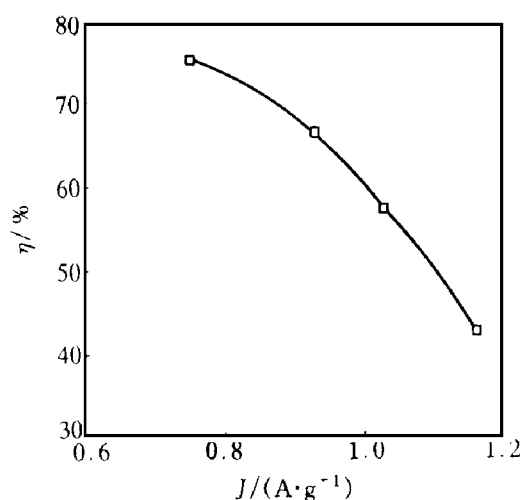


Fig. 5 Relationship between high rate dischargeability and exchange current density (J) of MH electrode

3.2.3 Charge retention of MH electrodes

The charge retention is also one of important characteristics of MH electrode. As shown in Table 5, the charge retention of MH electrodes increase with x decreasing. The fact is

caused by the fact that the equilibrium pressure decreases and the enthalpy change $-\Delta H$ value of metal hydride formation increases with x decreasing to make metal hydride more stable to suppress the self-discharge of MH electrodes.

Table 5 Effect of x on charge retention of MH electrodes

Alloys MmB_x	Charge retention/ %
$x = 4.4$	91.3
$x = 4.6$	90.5
$x = 4.8$	88.4
$x = 5.0$	87.4

REFERENCES

- 1 Iwakura C and Matsuoka M. Prog in Batteries and Battery Materials, 1991, 10: 81.
- 2 Iwakura C, Sakai T and Ishikawa H. Denki Kagaku, (in Japanese), 1992, 60: 680.
- 3 Matsuoka M, Asai K, Fukumoto Y *et al.* J Alloys and Comp, 1993, 192: 149– 151.
- 4 Tang Z Y, Chen W X, Liu Z L *et al.* J Applied Electrochem, 1996, 26: 1201.
- 5 Chen W X, Tang Z Y, Guo H T *et al.* Acta Physico-Chimica Sinica, (in Chinese), 1996, 12: 704.
- 6 Iwakura C, Fukumoto Y, Matsuoka M *et al.* J Alloys and Comp, 1993, 192: 152– 154.
- 7 Wada M, Yoshinagn H and Kajita O. J Alloys and Comp, 1993, 192: 164– 160.
- 8 Nogami M, Tadokoro M, Kimoto M *et al.* Denki Kagaku, (in Japanese), 1993, 9: 1088.
- 9 Notten P H L and Hokkeling P. J Electrochem Soc, 1991, 138: 1877.
- 10 Nogami M, Tadokoro M, Kimoto M *et al.* Denki Kagaku, (in Japanese), 1993, 9: 1094.

(Edited by Huang Jinsong)